Phase contrast and interference microscopy with the electron microscope

By P. N. T. Unwin

Medical Research Council, Laboratory of Molecular Biology, Cambridge

[Plates 13 to 16]

A simple electrostatic device has been constructed which, when inserted in the optical system of an electron microscope, functions as an absorbing phase plate. Its operation depends on the central portion of a thin poorly conducting thread generating a stable potential under the influence of the electron beam and creating a particular form of electric field. An electron interference technique is employed to study the stabilizing mechanism and to develop a method for achieving the required magnitude of potential.

The performance of this device is gauged by optical diffraction of electron micrographs of a thin carbon film; its application is illustrated by examining some negatively stained biological specimens. The results indicate that such an 'electrostatic phase plate' can provide significant improvements in contrast and signal/noise ratio over normal bright field images without loss in resolution.

1. Introduction

Two types of contrast are involved in imaging biological materials in the electron microscope: amplitude contrast, which is accomplished by preventing some of the scattered electrons from reaching the image plane, and phase contrast, which is accomplished by introducing a path difference between the scattered and unscattered waves before allowing them to interfere. Of the two mechanisms, phase contrast dominates when the material is of molecular or atomic dimensions (Heidenreich 1964; Heidenreich & Hamming 1965; Eisenhandler & Siegel 1966).

Optimal defocusing is the current method of introducing the path difference necessary to achieve phase contrast. The method does however have its limitations: it is only effective for a small range of spatial frequencies, and it all too easily introduces artefacts into the image owing to contrast reversal effects. Furthermore, the maximum contrast achievable by defocusing is limited by the high intensity of the unscattered beam.

The present investigation is an attempt to overcome some of the drawbacks associated with defocusing by constructing a simple electrostatic phase plate to insert into the optical system. We may recall the remarkable success of the phase plate of light microscopy, introduced by Zernike in 1942. Unfortunately, although some success has been achieved at low resolutions (see, for example, Locquin 1954; Faget, Fagot & Fert 1960), no electron optical method analogous to Zenike's has yet been developed that provides similar improvements at the usual electron microscope working resolution of less than 1 nm.

The experiments are mainly concerned with the construction and testing of our particular type of phase plate; they include a study of potential distributions using an interference technique, an examination of the suitability of a certain form of electric field for producing the required phase shifts, and a study of the image of a thin carbon film to show that our device, when correctly constructed, can indeed produce the phase shifts that are required. To complete the investigation, some biological specimens are also examined with the phase plate in position, and a comparison is made between the 'phase contrast' image and the normal bright field image obtained by defocusing.

2. PROPOSED METHOD FOR PRODUCING PHASE CONTRAST

The primary requirement for good phase contrast in the image plane is that the optical path of the scattered wave front be changed relative to that of the unscattered wave front by a quarter of a wavelength ($\frac{1}{4}\lambda$) over a large portion of the area included by the objective aperture. An increase in the optical path of the scattered wave produces dark contrast—that is, makes more strongly scattering parts of the object appear darker. This is the type of phase contrast normally achieved by defocusing (weakening the lens) by small amounts. Our plan was to construct a device that produces the other type of phase contrast, bright contrast (making more strongly scattering parts of the object appear brighter), fulfilling the primary requirement by means of a specially shaped electric field. This device would be inserted in the back focal plane of the objective lens (where the electron diffraction pattern is formed) and made to partly obstruct the central order beam, thereby providing additional enhancement of contrast.

In considering the form of the field required, let us for the moment neglect the phase shifts introduced by, for example, spherical aberration and errors in focusing, and consider the phase shift created by an electric field centred at the intersection of the back focal plane with the optic axis. For a given type of field, this phase shift is simply $2\pi\lambda^{-1}C\beta\alpha(\beta)$, where C is a constant and $\alpha(\beta)$ is the deflexion, by the field, of electrons scattered by the specimen at an angle β to the direction of the incident beam. Now if the field is a cylindrical one, the phase shift (in the direction normal to the cylindrical axis) works out to be proportional to β, since $\alpha(\beta)$ is independent for β for the small deflexions being considered (Möllenstedt & Düker 1956); similarly, if the field is a spherical one, the phase shift (for all azimuths) can be shown to be independent of β. On this simple reasoning we could imagine a short charged cylinder positioned in the path of the central order beam producing the desired phase shifts: the field would be roughly cylindrical to a radial distance corresponding to half the length of the cylinder, giving a small but increasing phase shift, and more nearly spherical thereafter— phase shift constant. Only close to the edge of the objective aperture, where spherical aberration effects become important and the lines of force converge, would we no longer expect the constancy of the latter phase shift to be preserved.

Preliminary experiments suggested that a practical device could be constructed along these lines by suspending a thin poorly conducting cylinder—in our case a spider's thread—over a circular aperture and allowing it to charge up under the electron beam; it is the possibility and effectiveness of such a device that we propose to investigate.

3. EXPERIMENTAL DETAILS

All experiments were performed with a Philips EM 300 electron microscope operating at 100 kV and fitted either with a goniometer or high resolution stage (objective lens focal length, $f = 1.6$ mm, spherical aberration coefficient, $C_s = 1.6$ mm).

The microscope was modified to produce interference fringes for the experiments described in the following section, and this was done by suspending the thread of a small spider ($\sim 0.3\ \mu$m in diameter) over a 2 mm diaphragm mounted in the selected area diffraction aperture holder and operating the microscope in the diffraction mode. To observe the interference fringes in good contrast the two condenser lenses were strongly excited so that a greatly demagnified image of the cathode crossover was produced at the back focal plane of the objective lens. This

image acted as the effective source for the thread-interference biprism, located a further 4 cm down the microscope column. The smallest diameter of the effective source which was commensurate with a reasonable magnification and exposure time was about 60 nm, indicating that the beam could be made sufficiently coherent to produce interference fringes to an extent of about 1 μm on either side of the thread with the microscope operating under optimum conditions. The fringes were focused in the object plane of the intermediate lens by having the diffraction lens (immediately below the thread) only weakly excited. A normal microscope specimen can also be focused in this plane by adjusting the objective lens current, so that, if desired, the microscope can now be used as a true interference microscope of the sort built by Fert, Faget, Fagot & Ferré (1962).

The standard high resolution stage was fitted when using the microscope as a conventional or phase contrast microscope, and to obtain sufficient accuracy in focusing all micrographs were taken at an electron optical magnification of 142000. The corresponding exposure times were up to 4 s with Ilford Special Lantern Contrasty plates. To ensure that optimum conditions for phase contrast would be realized, a 100 μm diameter second condenser aperture was employed, giving a minimum transverse coherence length of 4 to 5 nm, and the height of the objective aperture/phase plate was adjusted to lie more or less exactly in the back focal plane. A three-bladed anticontaminator was also designed so as to surround both the objective aperture/phase plate and the specimen. Used in conjunction with an aperture holder, modified to maintain a temperature of 120 °C at the optic axis, this device appeared to eliminate completely any observable residual astigmatism associated with either the phase plates or the normal objective apertures.

4. INTERFERENCE MEASUREMENTS

Having placed a spider's thread in the biprism position of the interference microscope described in §3, observation of its interference pattern indicates that one of two situations may be realized on illuminating it: its potential may either increase rapidly and continue to do so in an uncontrollable fashion, or else may quickly attain a certain value at which it stabilizes. The former is the case when the beam fails to touch the supporting diaphragm and the latter the case when it does touch. The beam does not, however, have to touch the diaphragm in the region where the diaphragm is contacted by the thread for stable fringes to be observed, and any mechanism accounting for the stabilizing process in terms of conductivity of the thread must therefore be discounted. A more likely explanation is that when the potential on the thread reaches a sufficiently high value the number of secondary electrons escaping from it is balanced by the number of secondaries, emitted from the diaphragm, that it captures. The possibility of other replacement processes such as leakage of current along the thread or capture of electrons from other sources should not be ruled out, but the capture of the slow-moving secondary electrons from the diaphragm is evidently the dominating mechanism. Curtis & Ferrier (1969) have advanced a similar argument in accounting for the 'bee swarm' effect in a collodion film.

The above mechanism implies that for a given illumination geometry the stabilizing potential should be independent of the beam intensity. Furthermore, the higher the ratio, R, of the electron flux on the thread to the integrated flux on the diaphragm, the higher should this stabilizing potential be. The first point can be demonstrated simply by varying the emission current and observing the constancy of the interference fringe spacing. The features illustrated in figure 1 demonstrate the importance of R. In figure 1a, plate 13, R has been made small, and

the interference pattern, in resembling the diffraction pattern of a thin cylinder, indicates a near-zero potential; in 1 *b* *R* has been increased so that closely spaced interference fringes are formed, indicating a high positive potential; in 1 *c* the intensity of the illumination has been varied along the thread to give a varying *R*, and the change in fringe spacing shows a definite correspondence between beam intensity and thread potential. The variation of potential along the thread as a function of electron flux can in fact be determined quantitatively by calibrating with a metallized thread of the same diameter, to which a range of known potentials have been applied, and exposing onto plates having known characteristics. In some experiments of this sort, using a range 0 to 200 V, the potential was found to vary along the thread proportionately to the electron flux.

The above experiments confirm the practicability of achieving a stable potential distribution of a suitable form when an insulating thread is suspended over an aperture placed in the plane of the electron diffraction pattern: for the weakly scattering material we wish to examine, the high intensity of the central order beam would ensure that the potential at the middle of the thread would be high in comparison with other parts, and the regions of the specimen and the aperture irradiated by the primary and the scattered electrons would provide the secondary emission necessary for this potential to stabilize. The requirement now is that the potential at the middle of the thread can stabilize at the correct value of a few volts. With the bare thread alone too high an *R* value would normally be achieved for this potential to be realized. A way of overcoming this difficulty, however, is to evaporate a layer of gold onto the thread. The gold, which is a much poorer emitter of secondaries, serves to lower the effective electron flux on the thread and to trap many of the secondaries that would otherwise leave it. Moreover, providing it is less than $\sim$ 40 nm thick the gold forms a discontinuous film so that the poor conducting properties of the thread are retained. Figure 2, plate 13, shows some interference patterns produced by a thread coated with a $\sim$ 30 nm layer of gold. The fringe appearance in (*c*), which is a combination of the features shown in (*a*) and (*b*), was generated by focusing the beam in the central region then quickly overfocusing, taking care not to let the beam touch the supporting diaphragm. The fact that the particular potential distribution so created cannot have changed significantly during the 16 s exposure confirms that the thread is still a poor conductor. That sharp fringes can be photographed when the diaphragm is not contacted by the beam, as in this case, is probably in part due to the metallized thread ejecting secondaries (i.e. charging up) at a much slower rate than would the bare thread alone, and in part due to the relatively greater importance assumed by replacement processes other than the capture of secondaries ejected from the diaphragm.

5. Estimating the phase shifts

Having established how to create an electric field centred on the optic axis that is both stable and of the correct magnitude, the next step is to determine more precisely the form of the field which is the most effective in producing the desired phase shifts. A method for doing this is as follows. A film containing markers (e.g. specks of evaporated metal) is mounted in the microscope in the normal specimen position, and at a distance Z ($Z < f$) below it is placed a thread-aperture combination as in figure 3. These are then illuminated under conditions similar to those encountered in the back focal plane of the objective lens (the required illumination conditions can be achieved simply by mounting a carbon film over the second condenser
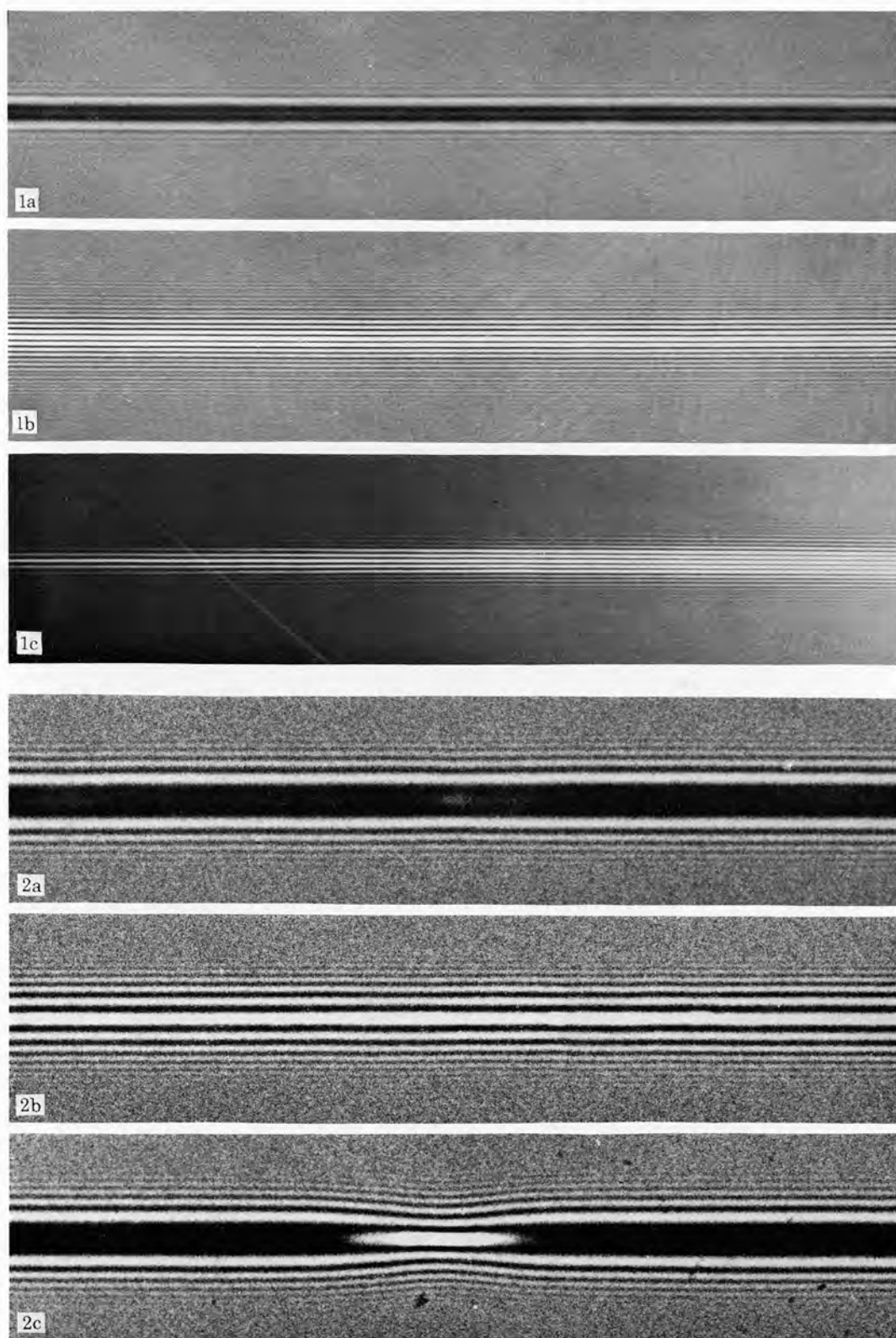
FIGURE 1. Interference fringes produced by a bare spider's thread under different illumination conditions. In (a) a substantial part of the supporting diaphragm surface was illuminated, in (b) only a small part was illuminated, and in (c) the thread was illuminated in a non-uniform manner. The corresponding interference patterns indicate a near-zero potential, a high positive potential (~ 200 V), and a potential that varies according to the beam intensity.

FIGURE 2. Interference fringes produced by a spider's thread coated with a ~ 30 nm thick layer of gold. A near zero potential is indicated in (a) and a positive potential of 9 V is indicated in (b). The pattern in (c) was obtained by focusing the beam on the central portion of the thread, then defocusing it to take the picture, ensuring at the same time that the supporting diaphragm remained unilluminated.
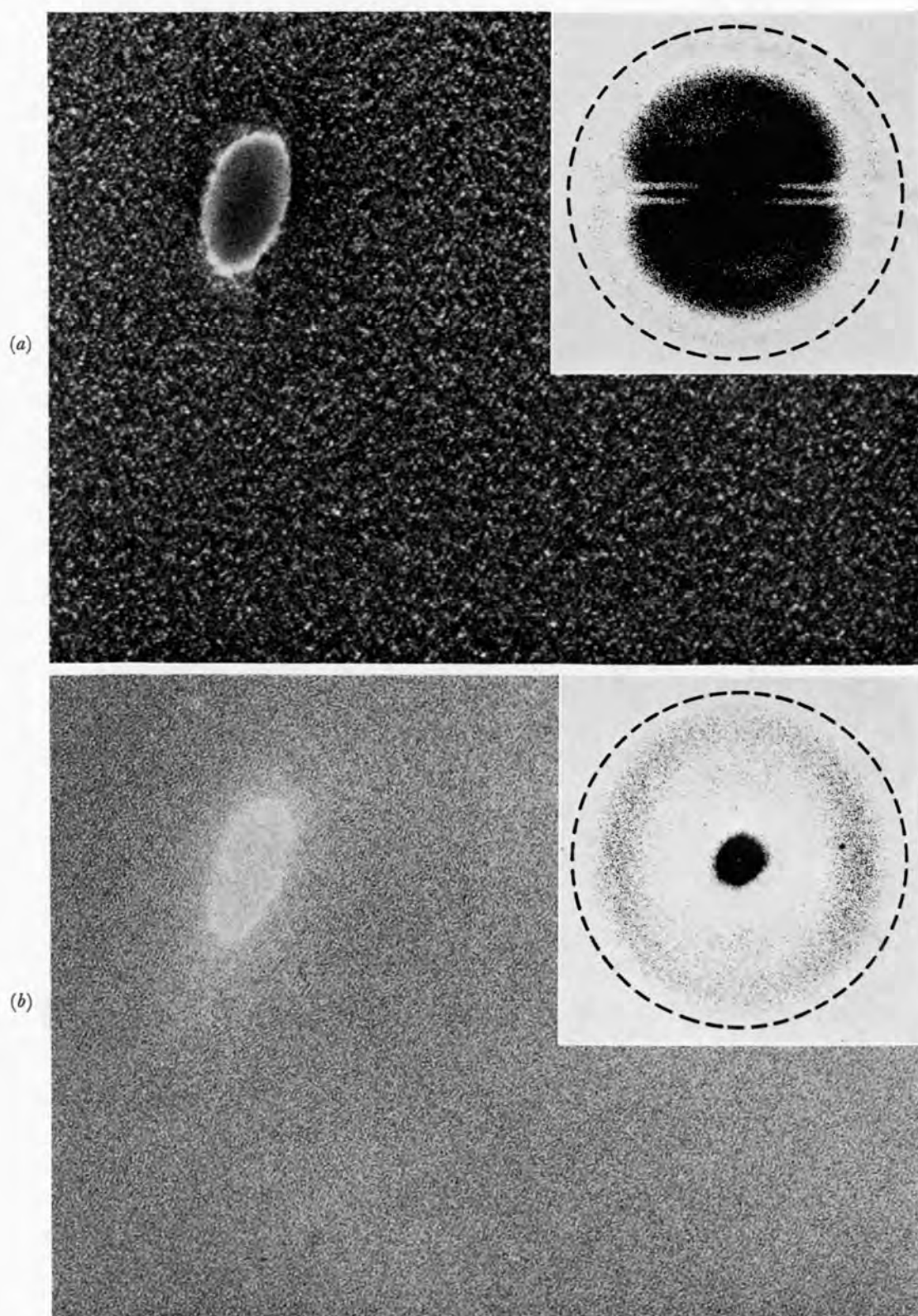
FIGURE 6. Micrographs and corresponding optical transforms of a thin in focus carbon film containing a hole. A phase plate having a 0.4 μm diameter thread and a 30 μm aperture diameter was used in taking (a) and a normal 30 μm objective aperture was used in taking (b). The scale of the optical transforms is indicated by the broken circles representing the aperture edges ($\beta = 9.4$ mrad.). (Magn. × 1 250 000.)
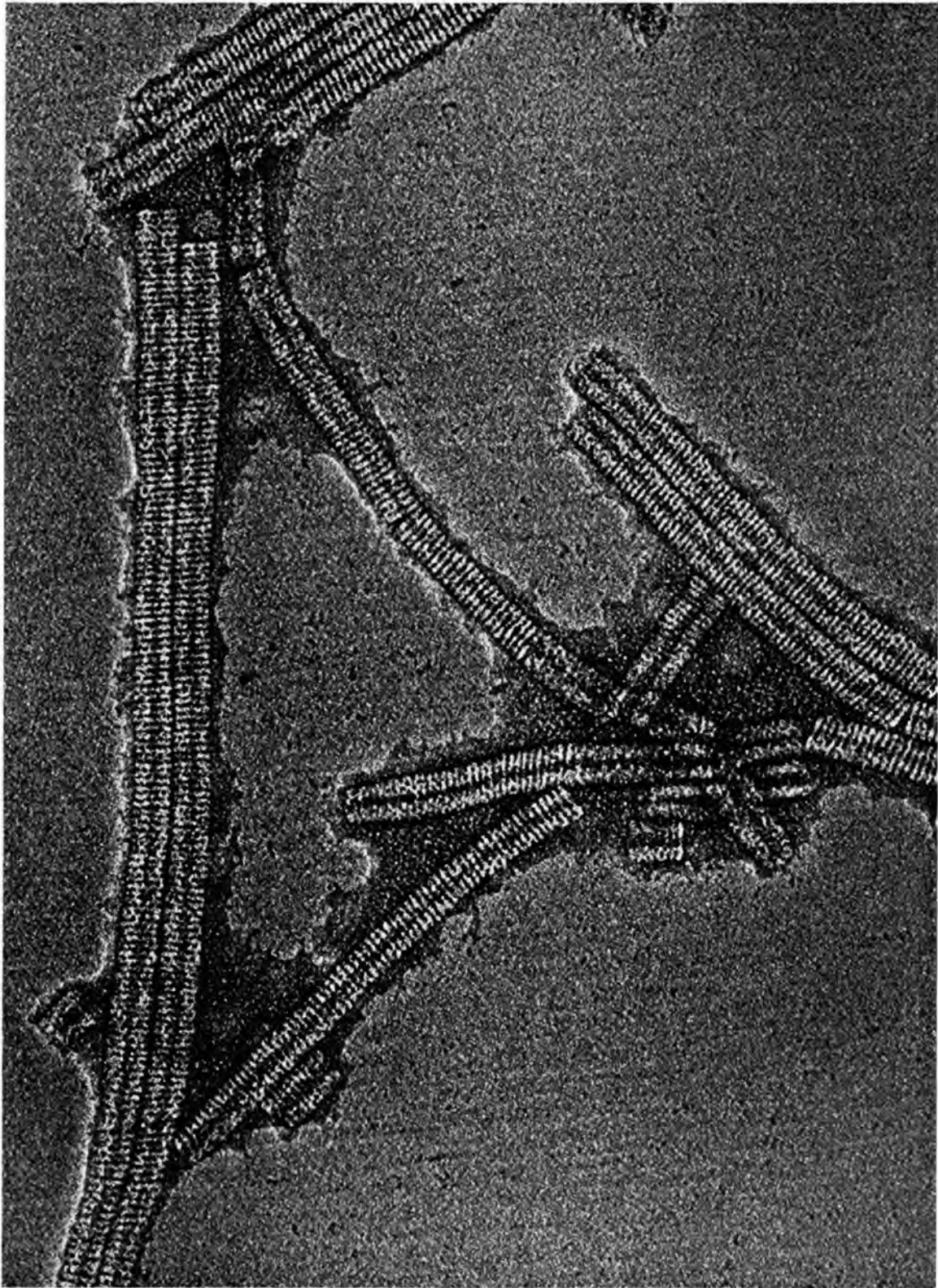
FIGURE 7. The rod shaped stacked disk aggregate of tobacco mosaic virus (TMV) protein stained in 1 % uranyl acetate and imaged with the phase plate in position. The rings of protein are $\sim$ 2.5 nm thick and $\sim$ 15 nm in diameter. (Magn. $\times$ 515000.)
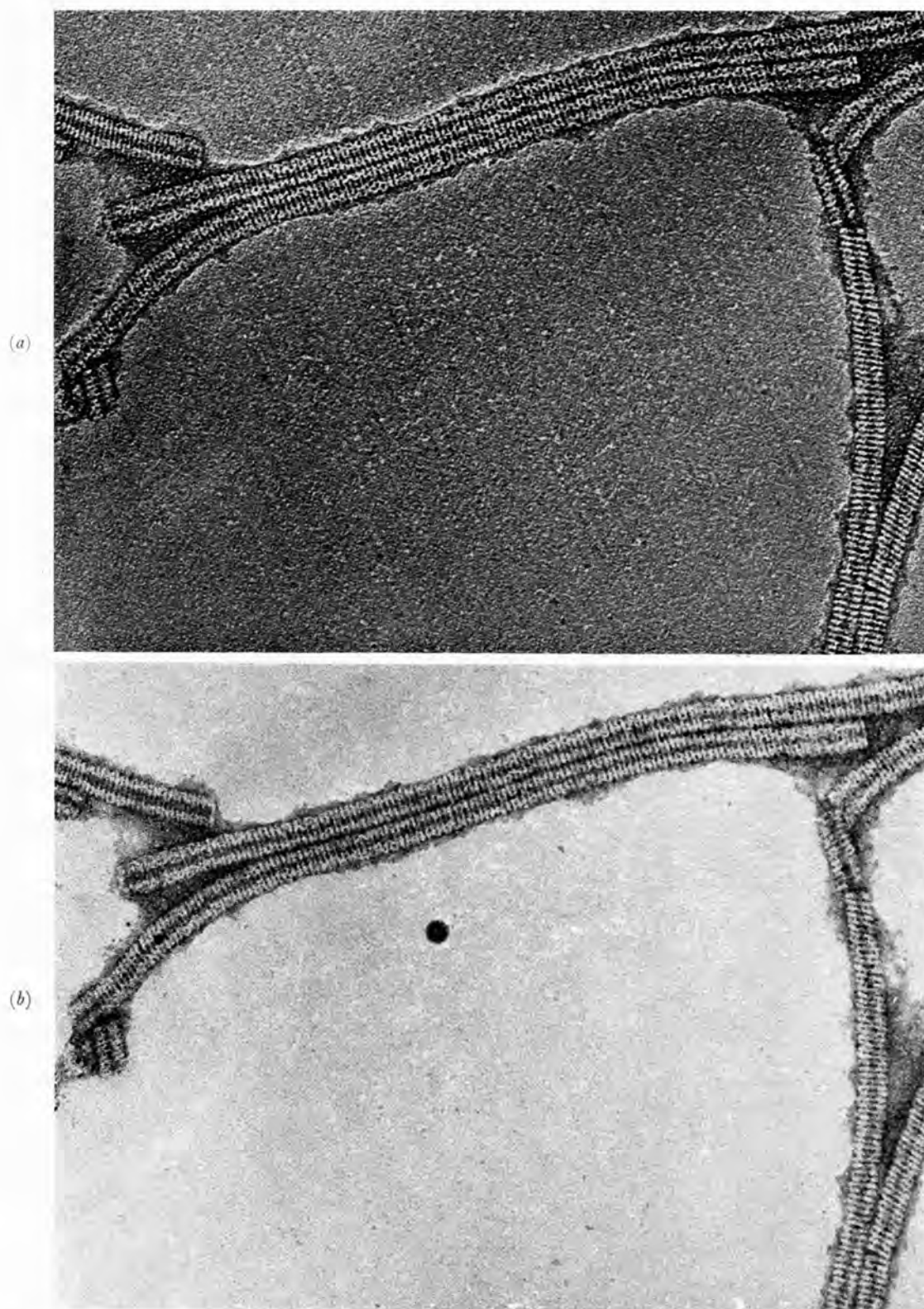
FIGURE 8. Comparison of (*a*) the bright contrast image taken with the phase plate in position and (*b*) the dark contrast image achieved by defocusing by about 100 nm. The specimens are the same as those in figure 7. (Magn. × 375000.)

aperture and focusing the second condenser lens to produce a small spot of high intensity at the middle of the thread; the focused beam simulates the relatively intense central order beam and the electrons scattered from the carbon provide the fainter background illumination of the remainder of the diffraction pattern). The image of the film containing markers becomes distorted as a result of the field generated by the thread, and by measuring the distortion at any point it is possible to calculate the deflexion of the electrons by the field directly below.
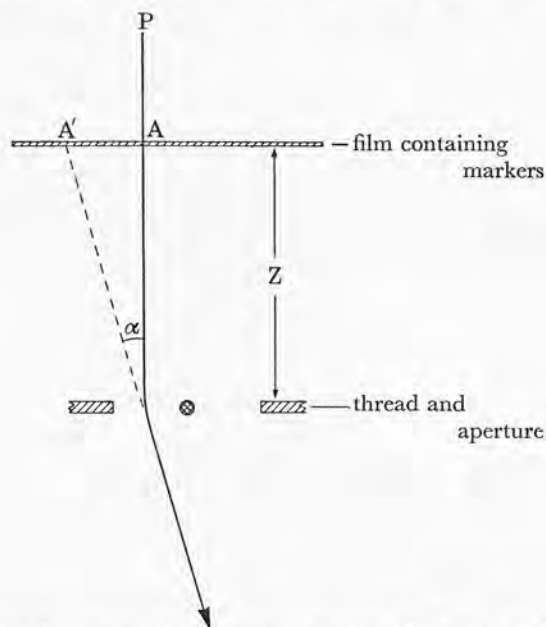

FIGURE 3. Diagram (not to scale) illustrating the method for measuring the deflexion of electrons by a thread-aperture combination. The deflexion, α, of electrons on path, P, makes point, A, on the thin film appear to come from point A', so that $\alpha \simeq AA'/Z$. Z is known and AA' can be measured by comparing micrographs of the film taken with and without the thread-aperture combination present.

Unfortunately, for easily measured distortions the maximum potential on the thread needs to be considerably higher than that which would be required when using the device as an actual phase plate. Nevertheless, the deflexions being considered are still small ($< 5 \times 10^{-4}$ rad) and the field potential is everywhere small compared to the accelerating potential. Simplification of the trajectory equation under these conditions indicates that if only the potential on the thread is changed the deflexions for all trajectories must be changed proportionately. Thus to deduce the optimum phase changes generated by a given geometry these measured deflexions can be scaled.

In a typical experiment of this sort Z was made 2.3 mm for an aperture of diameter 56 μm which supported a bare thread of diameter 0.6 μm, and the second condenser lens was focused to produce a 2 μm diameter beam of approximately uniform intensity at the centre of the thread. A thin carbon film over the second condenser aperture ensured that the illumination at the centre of the thread was well over an order of magnitude more intense than anywhere else. The thin film therefore ensured that the potential at other parts of the thread could be neglected in comparison, but necessitated a wide range of exposures for recording purposes. Figure 4 shows how the deflexion was found to vary along the radius perpendicular to the thread. Other deflexion measurements indicated that an approximately rotationally symmetrical field was achieved within the annulus bounded by the aperture edge and with an inner radius of ~ 2 μm.

P. N. T. UNWIN

As expected, this was not the case closer to the centre of the thread where the deflexions were more nearly perpendicular to the thread axis, rather than radial. The lack of rotational symmetry in this region indicates that a phase shifting device of this nature is bound to introduce astigmatism into the final image. However, this region is small in extent, indicating that such an aberration should only be encountered among the very low spatial frequency information.
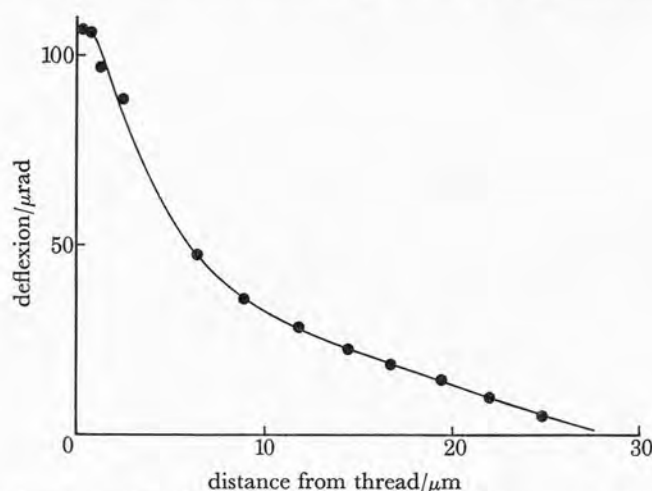

FIGURE 4. How the deflexion, α, was found to vary with distance from the centre of a thread-aperture combination under the conditions described in the text. The measurements were made in a direction perpendicular to the thread.
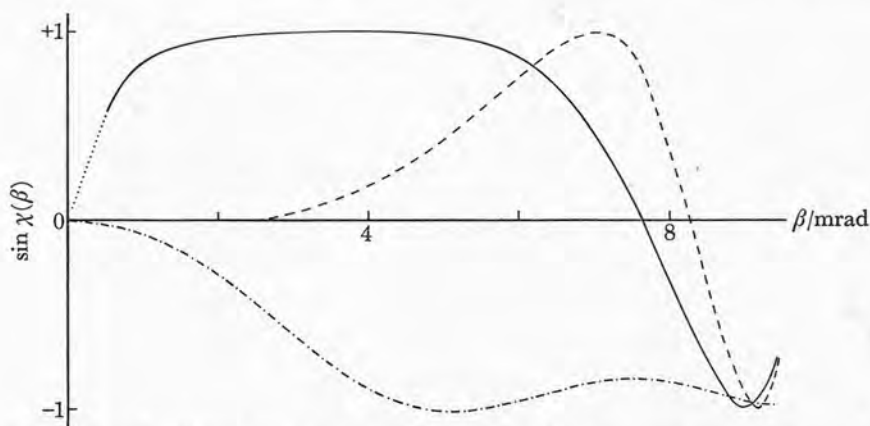

FIGURE 5. Phase factor, $\sin \chi(\beta)$, plotted as a function of scattering angle, β.——, experimental curve for optimum bright contrast with a phase plate in position; – – –, bright field, in focus; –·–, bright field, +90 nm defocus.

By scaling the data of figure 4 and assuming the total aberration phase shift in the rotationally symmetrical region to be given by

$$\chi(\beta) = 2\pi\lambda^{-1} \left(C\beta\alpha(\beta) + \tfrac{1}{4}C_{\mathrm{s}}\beta^4 \right)$$

we obtain an optimum $\sin \chi(\beta)/\beta$ distribution for bright contrast of the form indicated in figure 5 for a 30 μm diameter aperture, 0.3 μm diameter thread and a 1μm central order beam diameter. Also plotted in this figure for comparison are the phase contrast transfer functions for the in focus and +90 nm defocus bright field images, these being defined by

$$\chi(\beta) = 2\pi\lambda^{-1} \left(\tfrac{1}{4}C_{\mathrm{s}}\beta^4 - \tfrac{1}{2}\delta f\beta^2 \right),$$

where δf is the degree of defocus. A defocus of $+90$ nm gives about the maximum area under the sin $\chi(\beta)/\beta$ curve (i.e. the most favourable dark contrast), for the range of β considered, that it is possible to achieve through defocusing without introducing phase contrast reversal effects.

The experimental transfer curve is not completely realistic for small values of β ($\beta \lesssim 5 \times 10^{-4}$ rad) where it has an azimuthal dependence; even so, it is sufficiently well defined to substantiate the suggestions made earlier: the phase shift of the unscattered wave, for which $\beta \lesssim 3 \times 10^{-4}$ rad, is too small to be important, and there is a large flat portion corresponding to sin $\chi(\beta) \simeq +1$, indicating a decrease in optical path of the scattered wave by $\frac{1}{4}\lambda$ over a very wide range of spatial frequencies. Unfortunately the phase shift due to spherical aberration prevents the flat portion from extending further into the high angle region.

6. CONSTRUCTING PHASE PLATES

A simple procedure for constructing the phase plates was found to be as follows: latex spheres of a suitable diameter are spread over a slightly convex glass surface; about 0.5 μm thickness of silver is then evaporated onto the glass and the spheres blown away. Next, a small spider is placed on the glass, allowed to move, and then shaken off so that it hangs below on its thread. The thread is now wound in by rotating the piece of glass so as to make the thread pass over a different part of the silvered surface each revolution, the spider being jerked occasionally to prevent it from climbing up or to make it give out more thread. Having thus ensured that sufficient thread has been applied to have passed over a large proportion of the holes left by the latex spheres in the silver film, squares of film are cut out and floated off on water. A number of such squares are bound to contain apertures of the required geometry; these are selected, mounted in diaphragms and coated with gold using a rotary shadow caster to produce an even thickness around the threads. A simple way to gauge the correct thickness of gold is to examine a thin carbon film in the electron microscope with a phase plate in position, having the illumination adjusted as it normally would be for high resolution work—e.g. with the beam focused on the specimen, giving at the same time a 1 μm diameter central order spot of roughly uniform intensity. The thin carbon film is a good phase test object (see Thon 1966) and, if the thickness of gold is correct, it displays high contrast phase detail, in which points only 0.4 nm apart can be distinguished, when it is *in focus*. A more satisfactory method of indicating the correct thickness, is however, to compare the optical transform of the appropriate electron micrograph with the experimental transfer curve, as we shall now show.

The appearance of an in focus carbon film and its corresponding optical transform taken (*a*) with a phase plate of dimensions similar to those arrived at in §5, and (*b*) with a normal 30 μm aperture in position, is illustrated in figure 6, plate 14. The error in focusing is assumed to be small in both cases since the micrographs were taken in quick succession and the maximum in the ring of enhanced intensity in (*b*) corresponds closely to the calculated position of the spherical aberration peak for the bright field image. Now in comparing the optical transform of (*a*) with the transfer curve for optimum bright contrast in figure 5, we observe that both indicate good phase contrast over approximately the same wide range of spatial frequencies. Moreover, the position of the faint outer ring in this transform (corresponding to contrast reversal) and the position of the negative peak of the transfer curve practically coincide. Hence from the similarity between the predicted conditions for optimum phase contrast and the

actual conditions employed in obtaining figure 6*a*, it must be concluded that the correct thickness of gold (*ca.* 30 nm) had been applied to the phase plate that was used.†

The optical transform of figure 6*a* also serves to show that uniform phase contrast can be achieved with the phase plate in practically all directions. Some reduction in the phase information content of the final image is nevertheless inevitable simply due to the fact that the thread obstructs a proportion of the scattered electrons. Indeed, since the scattered beams have the same diameter as the unscattered beam at the thread, the amplitudes of all the scattered beams centred less than their radius away from the thread must be lowered. But note that, since the beam diameter is greater than the thread diameter, none of the scattered beams can be completely eliminated in this way. The obstruction effect is therefore not as detrimental to the image as it may at first appear.

The band of reduced intensity bisecting the transform can be accounted for on the above basis since it has a half width about equal to the sum of the radius of the thread and the radius of the beam at the thread. However, to account for the 'tramline' appearance of this band, it is necessary to consider an additional effect due to diffraction of the scattered electrons: we know from diffraction theory that each original sharp point in the object plane of the electron microscope is in fact blurred into a region the size of the aperture transform in the image plane. With a circular aperture this transform is, of course, the Abbe disk, which is very small. With the phase plate, on the other hand, the effect of the thread is to blur each point in the object into a long streak (*ca.* 40 nm in length for a 0.3 μm diameter thread) in a direction perpendicular to its axis. Fortunately, because the streak is spread out over a long distance and only a low proportion of Fourier components is affected, this diffraction effect does not degrade the image to any marked degree. Thus the sharpness of the edge of the hole in figure 6*a* is practically uniform around its circumference. Even so, we must expect to reconstruct the 'thread image' in the optical transform and clearly this image must lie symmetrically in the band, giving rise to a 'tram line' appearance. In addition, since the phase of the scattered electrons is not changed on diffraction by the thread, we might expect the intensity along the 'thread image' to vary in the same fashion as do other radii in the transform. In an exact analysis, however, some departure of the electric field from its ideal form close to the thread axis may well have caused the intensity to vary in a more complicated fashion.

7. Examining biological specimens

In taking micrographs with the phase plate in position the specimen must be accurately focused (the destructive effect of a defocus of only 90 nm can be readily appreciated from figure 5) and, if the oblique illumination effect characteristic of a schlieren image is to be avoided, the thread must also be accurately centred. Figure 7, plate 15, illustrates the appearance of a negatively stained biological specimen with these conditions fulfilled and using a phase plate that stops off about two-thirds of the unscattered electrons. At first sight the micrograph seems to differ very little from the image we might expect to achieve in bright field by defocusing a small amount. However, a closer look reveals that the thicker material of the specimen, rather than being slightly darker than the thin carbon support film, is much brighter. The contrast between the stain and the carbon film is also diminished. To explain these features it

† The values of such parameters as the thickness of the gold film, the thread diameter and the thickness of the carbon film are not in fact critical in producing the optimum phase shifts: some variation in the thread potential can be achieved by making small adjustments to the focusing of the two condenser lenses.

must be appreciated that, in preventing a portion of the unscattered electrons from reaching the image plane, there is an amplitude effect which is to make parts of the object that scatter more strongly into the aperture appear brighte than they would in the corresponding bright field image. With about two thirds of the unscattered beam stopped off, it can be shown that in this way the material of the specimen would become a little brighter than the thin carbon support film, but the stain would remain a little darker. Now bright phase contrast must reinforce this amplitude effect, especially for the parts of the object, such as the specimen itself, which scatter strongly into the aperture. There is, however, an important difference between the two contrast mechanisms, which is indicated in figure 5: phase contrast dominates for object spacings less than ~ 5 nm ($\beta = 7.4 \times 10^{-4}$ rad). We can therefore conclude that although the contrast in figure 7 is due to both amplitude and phase contrast effects, the enhancement of the fine detail of the actual specimen—which is our main concern—is mainly due to phase contrast.

To illustrate more clearly the differences between bright contrast achieved with the phase plate and dark contrast achieved by defocusing we will compare the two micrographs shown in figure 8, plate 16. These are of the same stacked disk aggregates of TMV protein taken (a) with the phase plate in position, and (b) in bright field at a defocus of 100 nm. To minimize any differences between the two due to irradiation damage, contamination, etc., the area was exposed to the full intensity of the electron beam for 40 s before either photograph was taken, and the delay between exposures was made less than 8 s.

To the eye, the most striking difference between the two micrographs is the greater contrast between the rings of protein and their subunits and the enhancement of the edges of the stain film in the bright contrast image. But in order to show the actual differences in a more quantitative fashion two sets of densitometer traces are reproduced in figure 9. These were taken along corresponding lines in the two micrographs perpendicular to the protein rings and along the optical transforms of corresponding areas in the direction indicating the disk repeat.

The first set of traces confirms that the enhanced contrast between individual rings in the image taken with the phase plate is a real effect. The reason for this improvement is believed to stem mainly from the relatively greater amount of phase contrast in the bright contrast image. In the first place, as can be seen from figure 5, this image has been constructed with better phase contrast transfer at lower spatial frequencies; the lower order Fourier components have therefore made a much more substantial contribution to the phase contrast than in the defocused bright field image. Secondly, the bright contrast image has been constructed with a greater proportion of scattered electrons: assuming two-thirds of the unscattered electrons were stopped off by the thread it is easy to show that the maximum phase contrast in this image should be greater by a factor of $\sqrt{3}$ over that achievable in bright field.

The second set of densitometer traces shows that the same intensities in the diffraction maxima corresponding to the disk repeat can be achieved using the phase plate, as in the bright field case, *without* the same large contributions from other maxima which are inconsistent with the specimen structure. In other words, the introduction of the phase plate has actually led to quite a marked increase in the strength of the wanted signal over that of the background noise. A simple explanation for this improvement is that whereas dark contrast in bright field more especially emphasizes the contrast due to the negative stain, bright contrast with the phase plate weakens this source of contrast and is more sensitive to the distribution of the material which the stain surrounds. In the former case the signal therefore derives mainly from

the stain distribution, but in the latter case it can be more closely linked to the actual specimen material. Any irregularities in the stain, due, for example, to its crystallization, must therefore have a less adverse effect on the signal:noise ratio of the bright contrast image. Equally important, the phase plate clearly provides more suitable imaging conditions for distinguishing between parts of the specimen which the stain has not been able to penetrate.
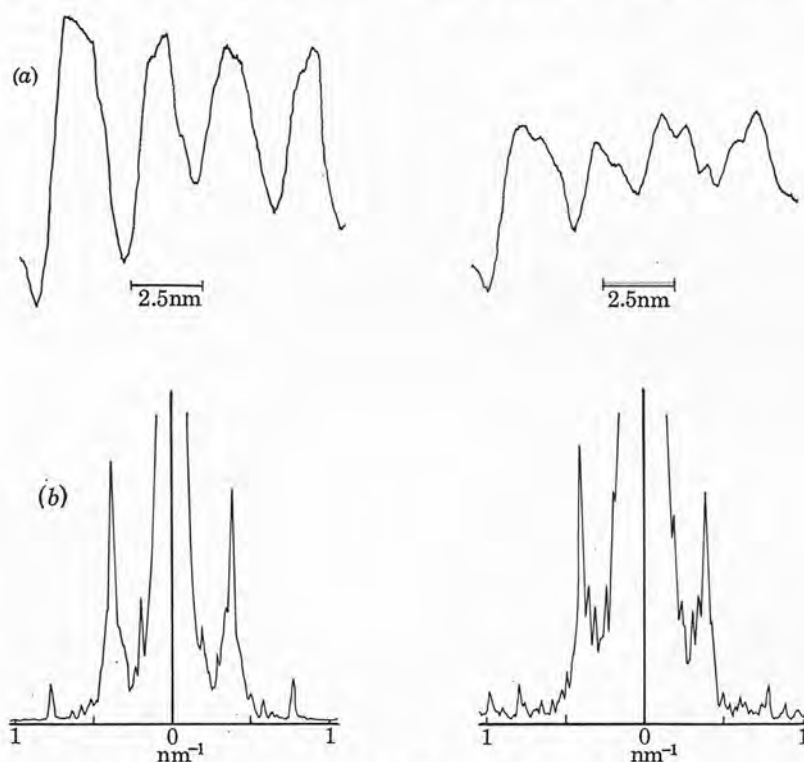
FIGURE 9. Densitometer traces of some features shown in figures 8 (a) and (b) illustrating improvements in contrast and in signal strength relative to background level in the bright contrast image. The traces in (a) were taken along corresponding lines perpendicular to the rings of protein, and the traces in (b) were taken along the optical transforms of corresponding areas in the direction indicating the disk repeat. The maxima due to the specimen structure are at approximately 0.2, 0.4 and 0.8 nm^{-1}. The traces for the bright contrast image taken with the phase plate are shown first in each case.

I am indebted to Dr H. E. Huxley, F.R.S., for his continued interest and for many helpful suggestions and criticisms; I would also like to thank Dr A. Klug, F.R.S., Dr P. W. Hawkes, Dr H. P. Erickson and Dr J. T. Finch for some invaluable discussions.

REFERENCES (Unwin)

Curtis, G. H. & Ferrier, R. P. 1969 Br. J. appl. Phys. 2, 1035.
Eisenhandler, C. B. & Siegel, B. M. 1966 J. appl. Phys. 37, 1613.
Faget, J., Fagot, M. & Fert, C. 1960 Proc. Reg. European Conf. on E.M. p. 18. Delft.
Fert, C., Faget, J., Fagot, M. & Ferré, J. 1962 J. Microscopie 1, 1.
Heidenreich, R. D. 1964 Fundamentals of transmission electron microscopy. New York: Interscience.
Heidenreich, R. D. & Hamming, R. W. 1965 Bell System Tech. J. 11, 207.
Locquin, M. 1954 Proc. Int. Conf. on E.M., London, p. 285.
Möllenstedt, G. & Düker, H. 1956 Z. Phys. 145, 377.
Thon, F. 1966 Z. Naturf. 21a, 476.
Zernike, F. 1942 Physica 9, 686.